An HA-based targeting system for improved lung cancer treatment

by

Shichen Li

BS, China Pharmaceutical University, 2024

Submitted to the Graduate Faculty of the

School of Pharmacy in partial fulfillment

of the requirements for the degree of

Master of Science

University of Pittsburgh

2024

UNIVERSITY OF PITTSBURGH

SCHOOL OF PHARMACY

This thesis was presented

by

Shichen Li

It was defended on

March 28, 2024

and approved by

Song Li, MD, PhD, School of Pharmacy

Xiaochao Ma, PhD, School of Pharmacy

Wei Zhang, PhD, School of Pharmacy

Thesis Advisor/Dissertation Director: Song Li, MD, PhD, School of Pharmacy

HA-based targeting system for improved lung cancer treatment

Shichen Li, MS

University of Pittsburgh, 2024

Non-small cell lung cancer (NSCLC) is the leading cause of cancer-related deaths worldwide. Platinum-based chemotherapy, such as cisplatin (CDDP), is a front-line treatment. However, the efficacy of platinum-related therapy is limited by the rapid development of drug resistance. Autophagy has been recognized as a critical factor in chemoresistance to CDDP. To overcome this, we introduced chloroquine (CQ) into the treatment, which is an effective autophagy inhibitor that can sensitize cancer cells to radiation and other anticancer drugs. To effectively co-deliver these two drugs, we developed a 5-aminosalicylic acid (5-ASA) derivatized nanocarrier based on hyaluronic acid (HA-ASA), which can actively target various types of cancer by targeting the overexpressed cell surface glycoprotein CD44.

We introduced 5-aminosalicylic acid (5-ASA) to the polymer (HA-ASA) as the hydrophobic core to form micelles. This novel nanocarrier can self-assemble in aqueous solution to form particles of ~100nm in size. Both CDDP and CQ can be loaded effectively into the HA-ASA micelles through various carrier/drug interactions with a final size of ~140 nm.

We showed that CDDP can induce autophagy in 3LL, FVBW17, and A549 cell lines and that the CDDP-CQ combination has a synergistic effect in vitro, with a combination index of smaller than 1. Meanwhile, we found that both CDDP and CQ can induce the expression of COX2, which can promote tumor progression, metastasis, and immunotherapy resistance. 5-ASA is an inhibitor of cyclooxygenase (COX), which can counteract the activity of the induced COX2.

The HA-ASA was shown to selectively accumulate in the tumor. This nanocarrier alone showed significant antitumor activity in the FVBW17 model. Codelivery of CDDP and CQ via 5-ASA-based polymer led to further improvement in antitumor activity. Studies are ongoing to investigate the impact of this combination therapy on tumor immune microenvironment *in vivo*.

Table of Contents

List of Tables

List of Figures

Preface

First and foremost, I want to thank my supervisor Dr. Song Li, the opportunity to work with him through my master's study is priceless. His devoted and hard-working personality inspired me in both research and personal fields, and his selfless support and guidance have encouraged me to dig deeper into science and explore new fields.

I would like to thank my thesis committee members, Dr. Xiaochao Ma and Dr. Wei Zhang for the precious time they have committed during this process.

I also want to thank Dr Haozhe Huang for sharing his knowledge and techniques with me, Dr. Yixian Huang for all the advice in chemistry. Thanks to all current and previous Li lab members, Dr. Jingjing Sun, Dr. Zhangyi Luo, Dr. Yuang Chen, Ziqian Zhang, Bei Zhang, Chien-Yu Chen, Yiqing Mu, Huatian Li, Sheida Dabiri, and Dr. Shangyu Chen, for their help and support.

Last but not least, I would like to thank my family for their unconditional support. Thank my father Xueming Li and mother Qiuyun Sun, for always trusting me and encouraging me to take all the challenges.

1.0 Introduction

1.1 Targeting autophagy is a potential strategy for solving chemo-resistance

Autophagy is a cellular process that removes damaged cell organelles, proteins, and other cellular debris. In this way, it helps cells to restore energy and is essential for overall cellular health and longevity. Autophagy has been linked to various physiological processes, including immunity, aging, and disease. It is assumed to provide energy for cancer cells under stressful conditions, and thereby, directly affects the invasion, metastasis, and proliferation of cancer cells, and can mediate the process of chemoresistance in the tumor microenvironment, which makes autophagy an attractive therapeutic target[1,2].

1.2 The wide use and limitations of platinum-based chemotherapy

Non-small cell lung cancer (NSCLC) is a subtype of lung cancer and accounts for up to 85% of it, which is the most frequent cause of cancer-related deaths worldwide[3-5]. Platinum-based chemotherapy is considered a front-line treatment for advanced NSCLC at present. The compound cis-[$Pt(NH_3)_2(Cl)_2$] (cisplatin, CDDP) was first described by Michele Peyrone in the 1840s, and in the late 20th century, it was confirmed that CDDP has antitumor activity. The therapy that involved CDDP was approved by the US Food and Drug Administration (FDA) in 1978. Cisplatin and its second-generation derivative, carboplatin, are alkylating agents that induce DNA damage and interfere with DNA repair[6,7].

However, acquired cisplatin resistance is always a problem for CDDP, leading to therapeutic failure[7].

1.3 Chloroquine, an autophagy inhibitor included in the drug combination

Chloroquine (CQ) is a long-used drug to treat malaria, and in past decades, accumulating evidence indicates that chloroquine has anti-autophagic activity and sensitizes cancer cells to radiation and other anticancer drugs. CQ contains weakly basic amines which tend to be highly concentrated in lysosomes. Within lysosomes, these compounds acquire a positive charge, become trapped, and alter the pH of endosomes or lysosomes, reducing their functionality. This interrupts the fusion of the autophagosome with the lysosome, and in this way, autophagy activity is decreased[8,9].

1.4 5-ASA as a COX-2 inhibitor to enhance the therapeutic effect

There is accumulating evidence indicating that cyclooxygenase (COX) plays an important role in tumor progression, metastasis, and immunotherapy resistance. Therefore, COX inhibition may be a key perspective for cancer therapy. Chronic inflammation is a risk factor for various types of cancers[10]. Prostaglandin E2 (PGE_2), a prostanoid lipid derived from the action of cyclooxygenases, plays a predominant role in promoting inflammation and tumor progression by regulating downstream targets that control cell proliferation, angiogenesis and immunosuppression[11]. COX-1 and 2, critical for the production of PGE2, are upregulated in

various malignant tumors, including colorectal, breast, stomach, lung, and pancreatic cancers[12,13]. Also, when treated with chemo drugs, The expression level of COX2 will be upregulated. Moreover, COX-2 overexpression is indicative of a poor outcome and recurrence[14], low survival rate immune escape[15,16], and resistance to cancer immunotherapy [17].

In this study, 5-aminosalicylic acid (5-ASA), a COX inhibitor was included in our combination therapy to counteract the activity of CDDP/CQ-induced COX 2.

1.5 HASA is an ideal carrier for the co-delivery of CDDP and CQ

If we use these drugs separately, the biodistribution may be different and we cannot achieve a good synergistic effect. So here we reported a delivery system. Hyaluronic acid (HA), when conjugated with the hydrophobic drug 5-ASA, can form self-assembled micelles.

We developed innovative hyaluronic acid (HA)-based nanocarriers (HASA) for effective codelivery of these drugs to prostate tumors. HA occurs naturally in living things, and it is the natural ligand of the CD44 receptors, which are overexpressed in tumors[18]. Through CD44-mediated transcytosis in tumor endothelial cells (ECs)[19,20], this delivery platform is highly effective in tumor targeting.

1.6 Overview of Thesis

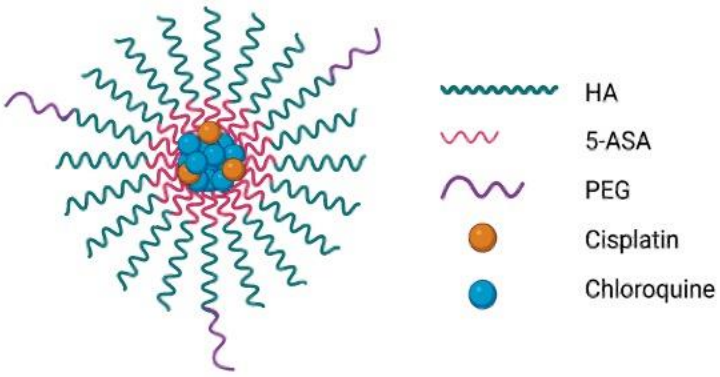

Figure 1 Overview of HASA/CDDP/CQ micelle

2.0 Methods

2.1 Material

Dulbecco's Modified Eagle's Medium (DMEM), RPMI 1640 Medium, trypsin-EDTA solution, 3-(4,5-dimethylthiazol-2-yl)-2,5-diphenyl tetrazolium bromide (MTT) and silver nitrate were purchased from Sigma-Aldrich (MO, U.S.A). Fetal bovine serum (FBS) and penicillin-streptomycin solution were purchased from Invitrogen (NY, U.S.A). 5-ASA was purchased from Frontier Scientific (UT, U.S.A). cis-diamminedichloroplatinum(II) (CDDP) was purchased from Chem-Impex (IL, U.S.A). Antibody against COX2, LC3 was purchased from Cell Signaling Technology, Inc. (MA, U.S.A). SuperSignalTM West Fento Maximum Sensitivity Substrate Kit and PierceTM RIPA buffer were purchased from Thermo Scientific (MA, U.S.A).

2.2 Animals and Cells

Female FVB/N mice (4–6 weeks) and female C57BL/6J mice (4-6 weeks) were purchased from The Jackson Laboratory (ME, U.S.A). All animals were housed under pathogen-free conditions according to AAALAC (Association for Assessment and Accreditation of Laboratory Animal Care) guidelines. All animal-related experiments were performed in full compliance with institutional guidelines and approved by the Animal Use and Care Administrative Advisory Committee at the University of Pittsburgh.

Murine lung cancer cell line 3LL, human lung cell line A549 was obtained from ATCC (VA, U.S.A). FVBW-17 murine lung cancer cell line[21] was kindly gifted by Professor Timothy Burns's lab at the University of Pittsburgh, Hillman Cancer Center. All cell lines used in this work were cultured in DMEM medium supplemented with 10% FBS and 1% penicillin/ streptomycin at 37 °C in a humidified atmosphere with 5% CO_2.

2.3 Synthesis of the HASA polymer

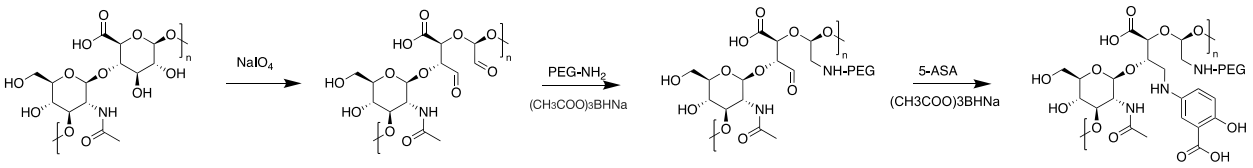

Figure 2 The synthesis route of HASA

Fig. 2 shows the synthesis scheme for HASA polymers. Different HASA polymers will be synthesized that vary in the degrees of 5-ASA and PEG2000 substitution. HASA was synthesized via the oxidation of HA (425mg, 1mmol) by $NaIO_4$(107mg, 0.05mmol) in 10 ml water, stirring at room temperature (RT) overnight, then dialysis in water for 48 and lyophilized. Then the HA-COOH and PEG-NH_2 were dissolved in 150 ml of water, add drops of HAc, and stirring for 24h at RT. Then 5-ASA (459mg, 3mmol) was added and stirred for another 24h. By adding different amounts of PEG2000 amine, different HASA can be synthesized. and 5-ASA to the aldehyde groups.

Chemical characterizations will include NMR and UV.

2.4 Preparation and Characterization of the Micelles

To prepare the PASA/CDDP micelles, CDDP solution (30mg, 100 μmol) was first mixed with silver nitrate (34mg, 200 μmol, 2 equiv.) in deionized water, followed by vigorous stirring for 4 h at room temperature in the dark. After silver chloride precipitation was removed by centrifugation, the aqueous solution of cis-diaminodihydroxyplatinum(II) complex was obtained. Then cis-diaminodihydroxyplatinum(II) complex was mixed with HASA solution (10mg/ml in water) at different polymer/drug weight ratios to give HASA/CDDP micelles. To prepare HASA/ CQ and HASA/ CDDP/CQ micelles, CQ solution (10mg/ml in DMSO) was mixed with HASA or HASA/CDDP solution. The concentration of CDDP or CQ was measured by o-phenylenediamine spectrophotometric method or HPLC-fluorescence detection method. The average diameter and the size distribution of micelles were assessed via a Zetasizer (DLS).

The CMC of HASA micelles was determined by plotting the light scattering intensity against the micelles' concentration, and the CMC was determined as the intersection of the best-fit lines drawn through the data points.

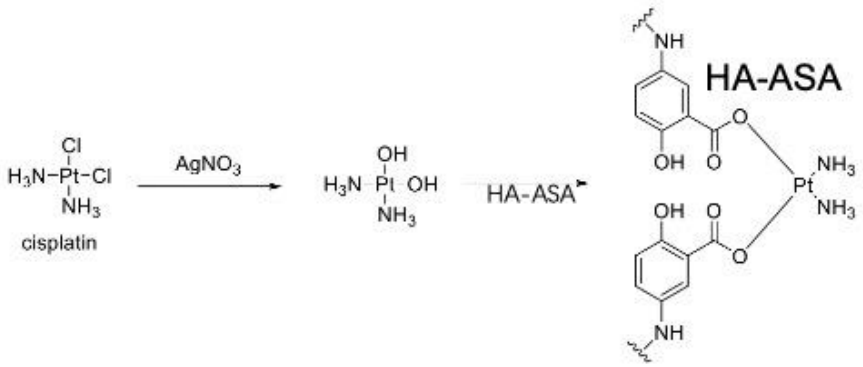

Figure 3 The interaction between HA-ASA and CDDP Coordinate bond

2.5 In Vitro Cytotoxicity Assay

Cytotoxicity assay was performed on the 3LL mouse lung cancer cell line, FVBW17 mouse lung cancer cell line, and A549 human lung cancer cell line. Cells were seeded in 96-well plates at various densities respectively ($3x10^3$ cells per well for 3LL,2 $x10^3$ cells per well for FVBW17, A549) followed by 24 h of incubation in DMEM or RPMI 1640 with 10% FBS and 1% streptomycin/penicillin.

To evaluate the combinational effect of CDDP and CQ, cells were treated with various concentrations of free CDDP, free CQ, and the combination of both respectively for 48 h before the MTT assay was performed.

MTT assay and the calculation of cell viability were performed as described before. The anti-proliferation data for single drug and combination treatment were fitted to an inhibitory, normalized dose-response model with variable slope (Y = 100/ (1 + 10^((LogEC50-X) *HillSlope); (GraphPad Prism, San Diego, CA)

2.6 Western Blot

Western blotting was performed to evaluate the COX2 and LC3 in 3LL, FVBW17 and A549 cells. Cells grown in six-wells plates with 80% confluency were treated with free CDDP, CQ, CDDP and CQ combination for 24 h. Cells were washed twice with pre-cooled PBS and lysed in PierceTM RIPA buffer for 2 h at 4°C. Protein concentrations were determined by the BCA method, and equal amounts of total protein lysate were resolved on a 10% SDS-PAGE and subsequently transferred to a nitrocellulose membrane. Membranes were blocked with 5% nonfat

milk in PBS for 1 h before incubation with rabbit anti-ASCT2 primary antibody dissolved in PBST (DPBS with 0.1% Tween 20) overnight at 4°C. The blots were washed with PBST and then probed with goat antirabbit IgG for 1 h at room temperature followed by chemiluminescence detection by SuperSignalTM West Fento Maximum Sensitivity Substrate. β-Actin or GAPDH was used as a loading control.

2.7 Evaluation of Autophagy

In addition, to evaluate the level of autophagy, an autophagy assay kit (MAK138) from Sigma-Aldrich was used in vitro according to the company datasheet. Cells grown in six-well plates with 80% confluency were treated with free CDDP, CQ, CDDP and CQ combination for 24 h, and then observed by laser confocal microscopy (CLSM, FluoView 1000, Olympus, Japan).

2.8 In vivo Biodistribution

DOX-loaded HASA micelles were prepared similarly to CQ-loaded HASA micelles at a HASA to DOX ratio of 10/1 (w/w). DOX-loaded HASA micelles were injected into 3LL tumor-bearing mice at a DOX dose of 10 mg/kg. At 24 hours, the mice were sacrificed, and major organs were dissected and subjected to imaging by the IVIS 200 system (Perkin Elmer, USA) at a 60s exposure time with excitation at 683 nm and emission at 703nm. Afterward, the organs were weighted and homogenized, and the DOX was extracted, then the concentration was tested by a

Waters 515 HPLC pump and a Waters 717 Plus Autosampler equipped with a Waters 2414 refractive index detector.

2.9 In vivo Therapeutic Study

Murine lung cancer FVBW17 model was established for in vivo antitumor efficacy study. FVBW17 cells (1×10^6 in 50 μL PBS) were inoculated s.c. at the flank of female BALB/c mice. When the tumor volume reached ~ 50 mm^3, mice were randomly divided into 5 groups (n=5), and treated via tail vein injection with mice were treated with PBS, the combination of CDDP and CQ, blank HASA, HASA/CDDP, HASA/CQ, and HASA/CDDP/CQ, every three days for a total of 5 times (HASA: 125 mg/kg, CDDP: 2.5 mg/kg, CQ: 25 mg/kg). Tumor sizes were measured with the digital caliper every three days following the initiation of the treatment and calculated by the formula: $(L\times W^2)/2$, where L is the longest and W is the shortest in tumor diameters (mm). Body weights were also monitored for the indication of toxicity. On day 23 post injection, all mice were sacrificed.

3.0 Result

3.1 Synergistic effect of CDDP and CQ

To assess the synergistic effect between CDDP and CQ, the proliferation inhibitory activity of CDDP and CQ, alone and combined, was examined on various lung cancer cell lines 3LL FVBW17 and A549. As shown in Fig. 3, CDDP and CQ alone showed a concentration-dependent inhibition of proliferation in all cell lines. It is also apparent that the combination of the two drugs could result in a significant improvement in the level of inhibition of cell growth. The combination Index was then calculated by CompuSyn. A synergistic cell-killing effect with a combination index (CI<1) between CDDP and CQ in 3LL(A), A549(B), and FVBW17(C) was observed. According to the CI, we selected the 1:5 mass ratio of CDDP to CQ in subsequent studies.

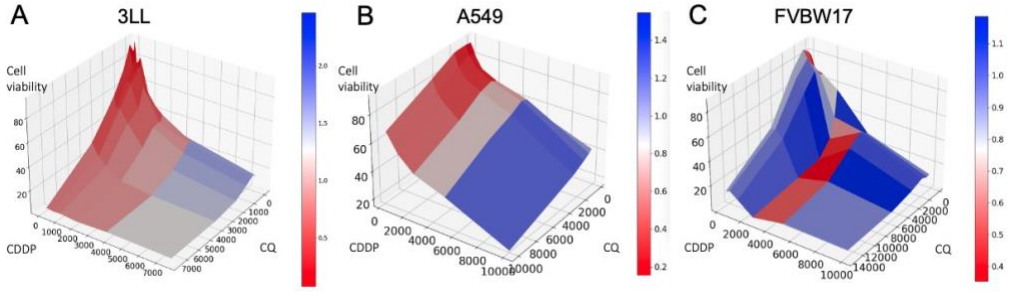

Figure 4 Synergistic effect between CDDP and CQ in inhibiting the proliferation of different lung cancer cell lines. (A-C) 3LL, A549, and FVBW17 cells were treated with various concentrations of free CDDP and CQ or a combination of them. After 48 h, the synergy score was calculated based on the MTT cytotoxicity assay. (n = 6 biologically independent samples). The red region in the figure represents the CI<1, which means there are synergistic effects at these concentrations of combined drugs, while the blue color represents the CI>1.**Synthesis and Characterization of the HASA micelles**

The HASA polymer was synthesized as shown in Fig.1. The ratio of 5-ASA was detected by UV (Fig. S1) and the ratio of PEG was detected by NMR (Fig S2). The PEG and 5-ASA contents were quantified in terms of molar ratio, i.e., the ratio of the number of units of HA to the number of molecules of PEG or 5-ASA. Table 1 shows that HASA polymers formed micellar particles of between 120 nm to 170nm, respectively. The CMC of HASA micelles was determined to be around 0.0052mg/mL. This relatively low CMC could help to maintain the good stability of the micelles upon being diluted in the blood bloodstream after intravenous administration and prevent the early release before reaching the tumor site.

Table 1 Characterization of HASA polymer

Ratio of input PEG	5-ASA Content	PEG Content	Size of Blank Micelle (nm)
0.05	0.2414	0.0203	140.1
0.1	0.2133	0.0385	127.9
0.15	0.2878	0.0646	160.4
0.2	0.2656	0.0817	166.5

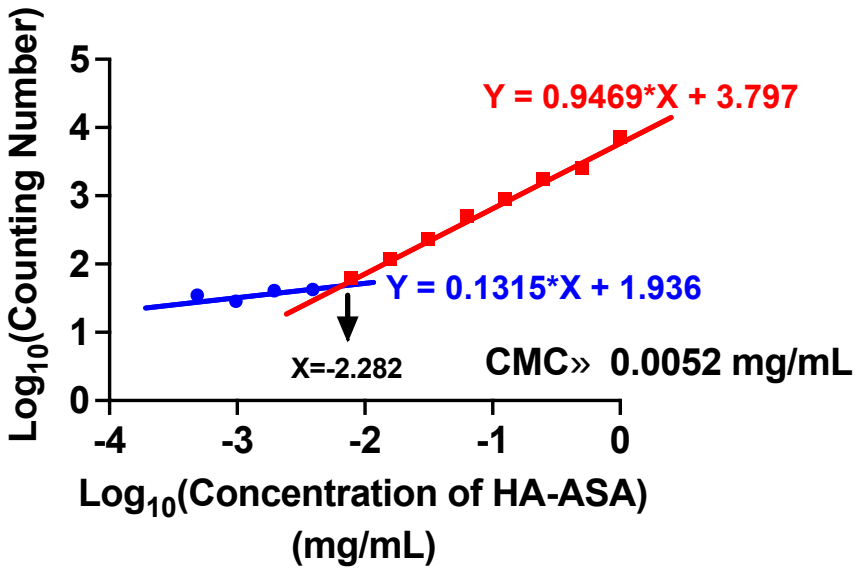

Figure 5 Measurement of Critical Micelle Concentration of HASA micelles

3.3 Drug Loading Test

The drug loading efficiency (DLE) was tested by using an ultra-filtration method. Table 2 shows the properties of drug-loaded HASA micelles at various carrier/drug ratios. The two drugs can be co-loaded, while hardly affecting the drug loading capacity.

Table 2 Characterization of HASA polymer

Micelles	Mass Ratio (mg:mg)	DLE (%)	DLC (%)
HASA:CDDP	10:1	81.2	8.12
HASA:CQ	10:1	89.3	8.93
HASA:CDDP:CQ	30:1:5	79.8:82.4	2.66:13.73

3.4 Expression levels of COX2 in drug-treated cells

To elucidate a potential role of tumor cells-derived COX-2 in 5-ASA-mediated antitumor activity, we examined the protein expression levels of COX2 in 2 cancer cell lines A549 (A) and 3LL (B). Both CDDP and CQ induced COX2 protein expression in a concentration dependent manner, and, when used together, the COX induction was even more significant.

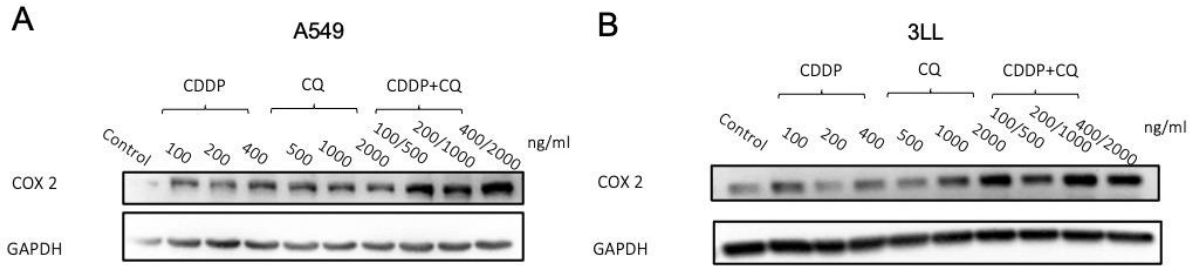

Figure 6 Expression of COX2 protein in CDDP and CQ treated cells. The expression level of COX2 has been upregulated after being treated with drugs in (A) A549 and (B) 3LL cell lines.

3.5 Induction of Autophagy

To look into the regulation of autophagy, we checked the expression of protein LC3II in 3LL, FVBW17, and A549 cell lines upon drug treatment. LC3 is one of the most important markers of autophagy, and when autophagy takes place, LC3 I will transfer to LC3II. As Fig.7 (B-D) shows, after being treated with CDDP, all the cell lines showed an upregulation of LC3II, which indicates that autophagy has been induced. 3LL cell line had a more significantly upregulated autophagy level when treated with CDDP, which somehow explains why it has the best response to the combination of CQ and CDDP. We also used the autophagy assay kit to check the signal from autophagosome and autolysosome, and the result was consistent with the expression at protein levels.

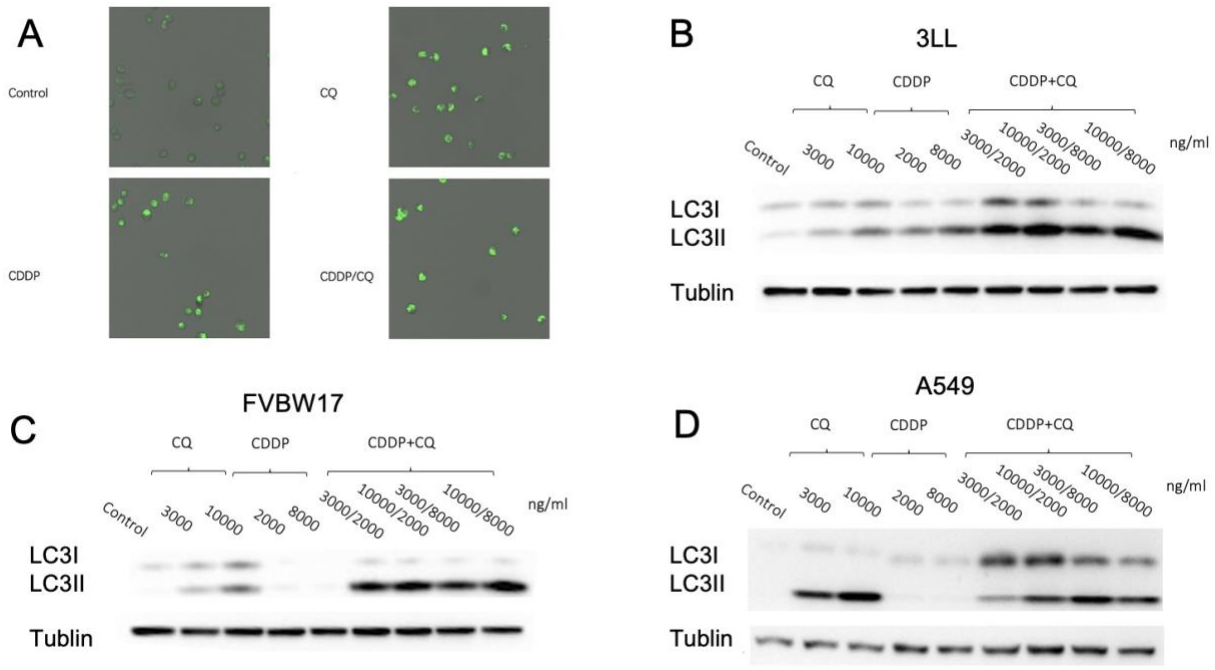

Figure 7 The induction and inhibition of Autophagy. (A) The green signal represents autophagosomes and autolysosomes (3LL) When treated with the acknowledged autophagy inhibitor CQ, the increased signal comes from the blocked flux resulting in accumulated autophagosomes. (B-D) The CDDP treatment can upregulate the expression of LC3II protein in 3LL, FVBW17, and A549 cell lines.

3.6 Biodistribution Study

The *in vivo* biofluorescence imaging was used for the assessment of the biodistribution of HASA micelles after systemic administration. DOX was loaded into HASA as the probe and then i.v. injected. Fig.8 shows the ex vivo imaging of tumors and other major organs that were collected from the mice. In addition to the fluorescent imaging, we conducted quantification to evaluate the delivery ability of the HASA carrier. The quantitative data shows that the HASA polymer with a

2% PEG modification can deliver more than 6% of the injected DOX to the tumor, which is consistent with the imaging data.

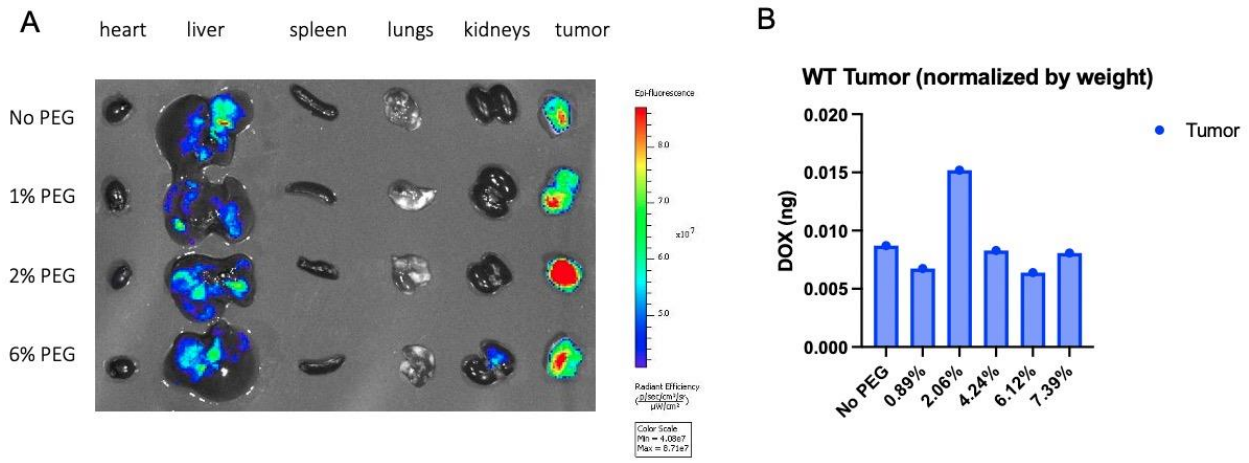

Figure 8 Biodistribution Study of HASA micelles. (A) The organ fluorescence image at 24 h after intravenous injection of DOX-loaded HASA micelle. (B) The quantification of DOX in the tumors.

3.7 In vivo Therapeutic Study

The in vivo tumor growth inhibitory activity of HASA/CDDP/CQ was investigated in a murine NSCLC model FVBW-17 (s.c. at flank). FVBW-17 is a novel tobacco-induced murine LUAD cell line with $Kras^{G12D}$ and Trp53 mutations, robustly representing human smoking-associated LUAD biology, and provides a much-needed preclinical model to evaluate new therapy. Blank HASA and the free drug combination showed minimal antitumor activity. Among all treatment groups, the HASA/CDDP/CQ group was most effective in inhibiting the tumor growth. All treatments were well tolerated as shown by similar body weights compared to control mice.

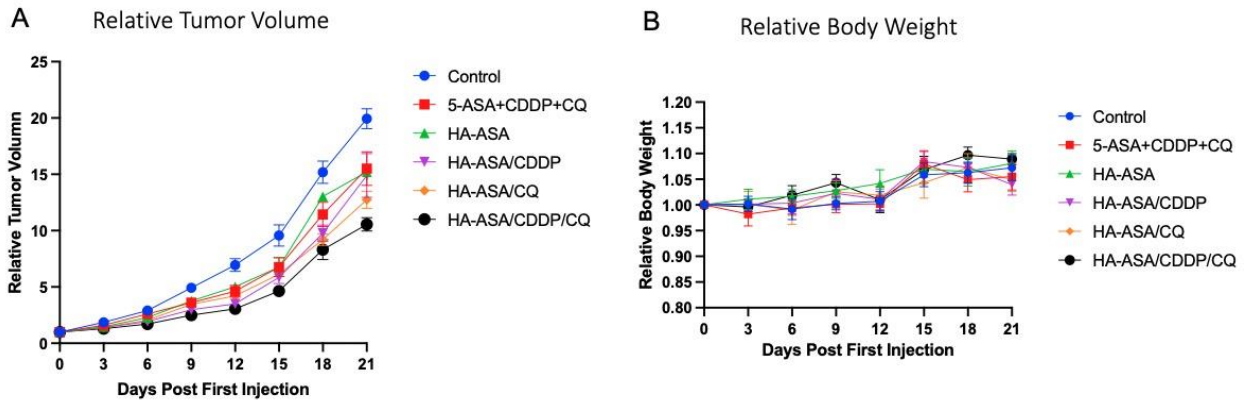

Figure 9 In vivo antitumor activity of HASA/CDDP/CQ micelle. (A) Blank HASA micelles, Free drug combination of CDDP, CQ and 5-ASA, CDDP loaded HASA, CQ loaded HASA, and the double drug loaded HASA via i.v injection in a murine breast cancer model (FVBW-17). Five injections were given every 3 days. (B) The weights of the mice in different treatment groups were measured every 3 days.

4.0 Discussion

In the past decades, autophagy has been studied as an impact factor in tumor development, including tumor initiation, progression, and response to therapy. It serves as a double-edged sword in cancer biology, exhibiting tumor-suppressive or pro-tumorigenic effects depending on the context and stage of tumor development. In the early stage of cancer, autophagy can exert tumor-suppressive effects by promoting the clearance of damaged cellular components and suppressing genomic instability. However, in the advanced stage, autophagy can promote tumor survival under stressful conditions, including exposure to chemo drugs and radiation, thereby contributing to tumor progression and therapeutic resistance.[9] Accumulating evidence has shown that in the advanced stage, inhibition of autophagy can sensitize cancer cells to chemotherapy-induced cell death, providing a rationale for combining autophagy inhibitors with front-line chemo drugs.[22,23] We have observed the synergistic effect both in vitro and in vivo, suggesting that it is a promising drug combination.

Targeted delivery systems can enhance the therapeutic effect of chemotherapies while reducing toxicity. The HASA delivery system is designed to utilize both the EPR effect and active targeting of the CD44 receptors, to achieve tumor targeting. Besides the delivery function of the, it also has antitumor activity as a 5-ASA prodrug. The COX inhibitors have been proven to improve the tumor microenvironments and suppress tumor growth. HASA, as a prodrug, can slowly release 5-ASA over a prolonged period to achieve sustained inhibition of COX. Our lab has previously developed a well-verified delivery system named PASA, which is also based on 5-ASA.[24] We have found that PASA-based treatment can improve the tumor microenvironment. And since it can increase the expression of PD-1 on the surface of $CD8^+$ cells, the combination of PD-

1 antibody and PASA/chemotherapy has potential. Based on the similarity between HASA and PASA systems, we are planning to detect the tumor immune environment after treatment and look into the combination of PD-1 antibody with HASA/CDDP/CQ system.

However, despite the promising outlook for this novel NSCLC treatment, there are still some interesting points to investigate. Specifically, we are interested in exploring the potential of this drug combination to reverse CDDP resistance, prompting further studies utilizing CDDP-resistant cell lines. Additionally, our observations suggest that the in vivo therapeutic efficacy may have been limited by the relatively low autophagy induction in the FVBW-17 tumor model. To address this, we plan to conduct studies using an alternative tumor model, such as 3LL, to broaden our understanding and optimize therapeutic outcomes.

Appendix A Supplemental Materials

Appendix A.1 Figures

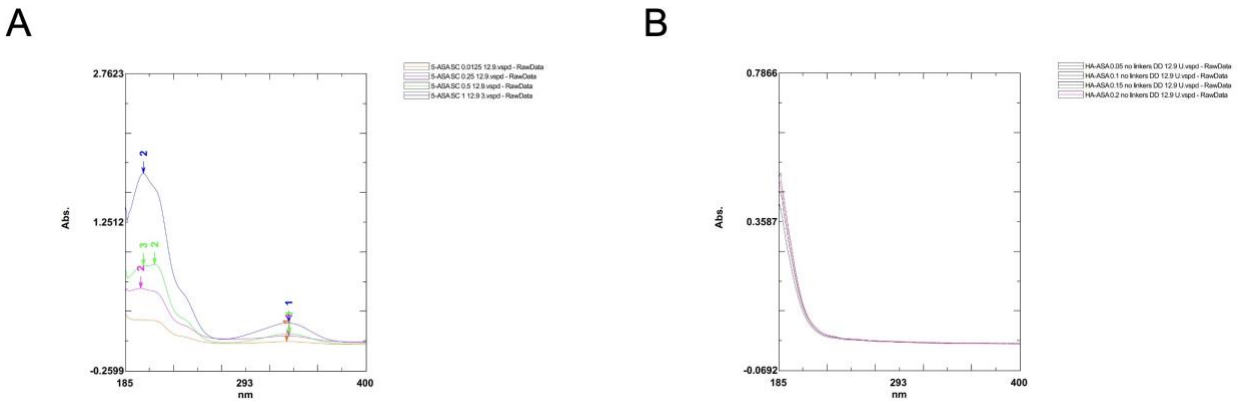

Figure S1 The UV absorbance spectrum of 5-ASA standard samples (A) and different HASA polymers(B)

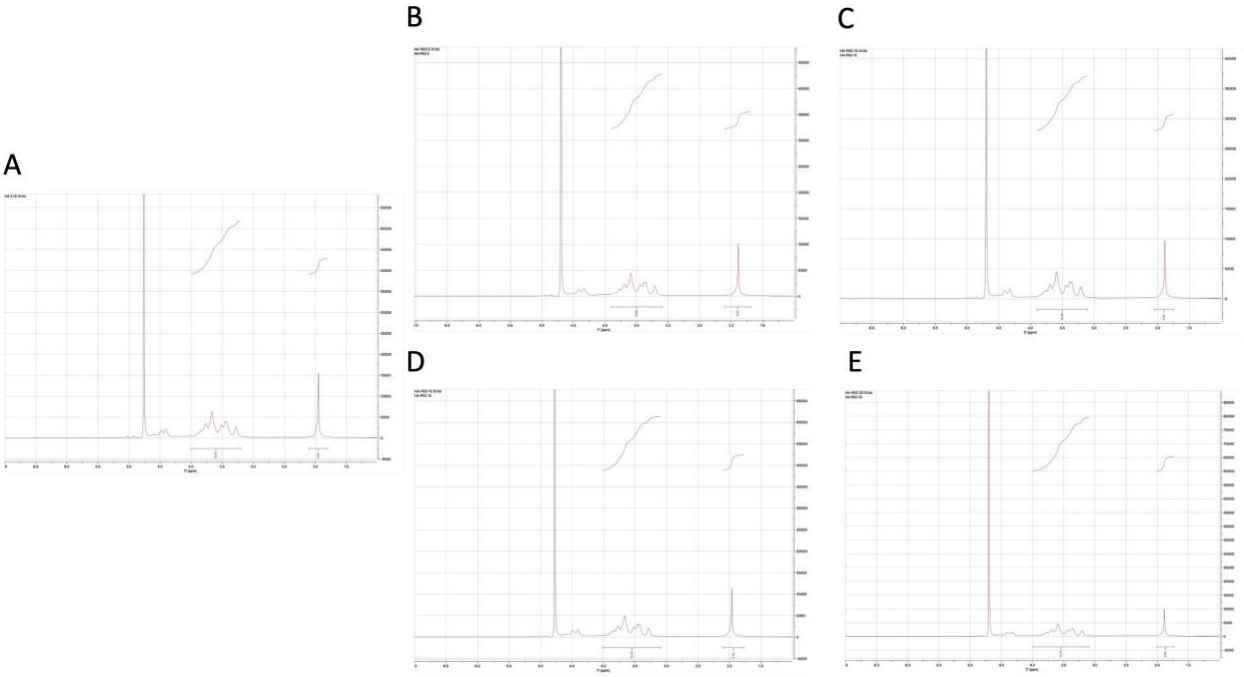

Figure S2 The ^{1}H-NMR of HA and different HASA polymers

HA (A), 5% (B), 10% (C), 15% (D), and 20% (E) PEG-modified HASA was tested by ^{1}H-NMR.

Bibliography

1 Mathew, R., Karantza-Wadsworth, V. & White, E. Role of autophagy in cancer. *Nature Reviews Cancer* **7**, 961-967 (2007).

2 Klionsky, D. J. *et al.* Autophagy in major human diseases. *The EMBO journal* **40**, e108863 (2021).

3 Gridelli, C. *et al.* Non-small-cell lung cancer. *Nature reviews Disease primers* **1**, 1-16 (2015).

4 Alexander, M., Kim, S. Y. & Cheng, H. Update 2020: management of non-small cell lung cancer. *Lung* **198**, 897-907 (2020).

5 Chen, P., Liu, Y., Wen, Y. & Zhou, C. Non‐small cell lung cancer in China. *Cancer Communications* **42**, 937-970 (2022).

6 Fennell, D. *et al.* Cisplatin in the modern era: The backbone of first-line chemotherapy for non-small cell lung cancer. *Cancer treatment reviews* **44**, 42-50 (2016).

7 Han, Y., Wen, P., Li, J. & Kataoka, K. Targeted nanomedicine in cisplatin-based cancer therapeutics. *Journal of Controlled Release* **345**, 709-720 (2022).

8 Mauthe, M. *et al.* Chloroquine inhibits autophagic flux by decreasing autophagosome-lysosome fusion. *Autophagy* **14**, 1435-1455 (2018).

9 Kimura, T., Takabatake, Y., Takahashi, A. & Isaka, Y. Chloroquine in cancer therapy: a double-edged sword of autophagy. *Cancer Res* **73**, 3-7 (2013).

10 Wang, D. & DuBois, R. N. Eicosanoids and cancer. *Nature Reviews Cancer* **10**, 181-193 (2010).

11 Song, W., Musetti, S. N. & Huang, L. Nanomaterials for cancer immunotherapy. *Biomaterials* **148**, 16-30 (2017).

12 Hangai, S. *et al.* PGE2 induced in and released by dying cells functions as an inhibitory DAMP. *Proceedings of the National Academy of Sciences* **113**, 3844-3849 (2016).

13 Zelenay, S. *et al.* Cyclooxygenase-dependent tumor growth through evasion of immunity. *Cell* **162**, 1257-1270 (2015).

14 Shi, C. *et al.* High COX-2 expression contributes to a poor prognosis through the inhibition of chemotherapy-induced senescence in nasopharyngeal carcinoma. *International journal of oncology* **53**, 1138-1148 (2018).

15 Peng, L., Zhou, Y., Wang, Y., Mou, H. & Zhao, Q. Prognostic significance of COX-2 immunohistochemical expression in colorectal cancer: a meta-analysis of the literature. *PloS one* **8**, e58891 (2013).

16 Rodriguez, N. I. *et al.* COX-2 expression correlates with survival in patients with osteosarcoma lung metastases. *Journal of pediatric hematology/oncology* **30**, 507-512 (2008).

17 Liu, B., Qu, L. & Yan, S. Cyclooxygenase-2 promotes tumor growth and suppresses tumor immunity. *Cancer cell international* **15**, 1-6 (2015).

18 Xu, H., Niu, M., Yuan, X., Wu, K. & Liu, A. CD44 as a tumor biomarker and therapeutic target. *Experimental Hematology & Oncology* **9**, 1-14 (2020).

19 Saravanakumar, G., Deepagan, V., Jayakumar, R. & Park, J. H. Hyaluronic acid-based conjugates for tumor-targeted drug delivery and imaging. *Journal of biomedical nanotechnology* **10**, 17-31 (2014).
20 Spadea, A. *et al.* Evaluating the efficiency of hyaluronic acid for tumor targeting via CD44. *Molecular pharmaceutics* **16**, 2481-2493 (2019).
21 Stabile, L. P. *et al.* Syngeneic tobacco carcinogen–induced mouse lung adenocarcinoma model exhibits PD-L1 expression and high tumor mutational burden. *JCI insight* **6** (2021).
22 Mulcahy Levy, J. M. & Thorburn, A. Autophagy in cancer: moving from understanding mechanism to improving therapy responses in patients. *Cell Death & Differentiation* **27**, 843-857 (2020).
23 Jain, V., Singh, M. P. & Amaravadi, R. K. Recent advances in targeting autophagy in cancer. *Trends in Pharmacological Sciences* (2023).
24 Huang, H. *et al.* A novel immunochemotherapy based on targeting of cyclooxygenase and induction of immunogenic cell death. *Biomaterials* **270**, 120708 (2021).